

Coulomb Final State Interaction in Pion Interferometry for the Processes of High Multiplicity

D.V. Anchishkin^{}1, W.A. Zajc^{**}, G.M. Zinovjev^{***}*

^{*}University of Jyväskylä, Department of Physics,
P.O.Box 35, FIN-40351 Jyväskylä, FINLAND
E-mail: ANCHISHKIN@jyfl.jyu.fi

^{**}Nevis Laboratories,
Columbia University,
Irvington, NY 10533, USA
E-mail: ZAJC@nevis1.nevis.columbia.edu

^{***}Bogolyubov Institute for Theoretical Physics,
National Academy of Sciences of Ukraine,
252143 Kiev-143, UKRAINE
E-mail: GEZIN@gluk.apc.org

Abstract

The corrections for two pion correlations due to electromagnetic final state interactions at high secondary multiplicities are investigated. It is shown that these result in a noticeable deviation from the standard Gamov factor. This conclusion changes drastically in a model of the pion system with expansion. The critical parameter which determines the size of these effects is found to be the ratio of the relative velocity of detected pions to the velocity of the pair center-of-mass (in the fireball rest frame). In particular, when this parameter is much less than unity the pion pair escapes the initial high density region promptly and the distortion of the mutual Coulomb potential is weak.

¹Permanent address: Bogolyubov Institute for Theoretical Physics, National Academy of Sciences of Ukraine, 252143 Kiev-143, UKRAINE (E-mail: ANCH@gluk.apc.org)

The fundamental observable for intensity interferometry in hadron physics is the relative momentum spectrum between two identical particles. For two like-charged pions, the final-state Coulomb interaction modifications to this spectrum result in a correction which has typically been considered to be tractable and relatively accurate. This expectation is based on the significantly different length scales between the strong ($\propto 1/m_\pi$) and the Coulomb ($\propto 1/m_\pi\alpha$) interactions in the problem [1, 2] (here m_π is a pion mass and α is a fine structure constant). In this case the the correction may be treated with the Schrödinger equation, resulting in the well-known Gamov factor $G(\mathbf{p}_1, \mathbf{p}_2)$. The nominal quantity expressing the correlation function in terms of experimental distributions [3]

$$C(\mathbf{p}_1, \mathbf{p}_2) = \frac{\langle n \rangle^2}{\langle n(n-1) \rangle} \frac{\frac{d^6\sigma}{d^3p_1 d^3p_2}}{\frac{d^3\sigma}{d^3p_1} \frac{d^3\sigma}{d^3p_2}}, \quad (1)$$

where $\langle n \rangle$ is the particle multiplicity, $d^3\sigma/d^3p$ and $d^6\sigma/d^3p_1 d^3p_2$ are the single-pion and two-pion cross sections, is then given (due to the factorization of the corresponding matrix element) in terms of the product of a Gamow factor multiplying the model correlations [4]

$$C(\mathbf{p}_1, \mathbf{p}_2) = G(\mathbf{p}_1, \mathbf{p}_2) C_{model}(\mathbf{p}_1, \mathbf{p}_2). \quad (2)$$

The standard derivation of the Gamov factor [5], obtained from the solution $\psi(\mathbf{r})$ of the nonrelativistic Schrödinger equation with the Coulomb potential, leads to

$$G(Q) = |\psi(0)|^2 = \frac{2\pi\eta}{e^{2\pi\eta} - 1}, \quad (3)$$

where

$$\eta = \eta_0 \equiv \frac{\alpha m_\pi}{Q}, \quad (4)$$

where Q is the relative momentum between the particles. It should be mentioned that, in terms of the pion momentum k in the pair center-of-mass, the relative pion momentum $Q = 2k$ coincides with invariant relative momentum $Q_{inv} \equiv [(k_1 + k_2)^2 - 4m_\pi^2]^{1/2}$ where k_1 and k_2 are pion four-momenta in an arbitrary frame. In order to better illustrate the more complicated cases discussed below, it is worthwhile to reconsider the calculation of this phenomenon as a quantum mechanical tunneling process (see for instance [6]).

In the quasi-classical approximation the probability for a pion of mass m_π starting from the point r_2 to reach the distance r_1 under the barrier is related to the quantity

$$\eta_{pen}(r_1, r_2) \equiv \frac{1}{\pi} \int_{r_1}^{r_2} q(r) dr, \quad (5)$$

with

$$q(r) = \left[2m_\pi \left(V(r) - E_{kin}^0 \right) \right]^{1/2}, \quad (6)$$

being the so-called “subbarrier quasi-momentum”. The equation $V(r_2) = E_{kin}^0$ determines the classical turning point.

For the pure Coulomb barrier $V_{Coul} = \alpha/2r$ the calculation of Eq. (5) gives

$$\eta_{pen}(r_1, r_2) = \frac{1}{\pi} [I(r_2) - I(r_1)], \quad (7)$$

with

$$I(r) = rq(r) - \eta_0 \arcsin \left[1 - 2 \frac{E_{kin}^0}{V_{Coul}(r)} \right], \quad (8)$$

where the factor of 1/2 in the potential accounts for the usage of the physical pion mass, not the reduced one, in Eq. (6). For penetration to $r_1 = 0$, corresponding to production of the two pions at the same space-time point, one obtains

$$\eta_{pen}(r_1 = 0, r_2) = \frac{\alpha m_\pi}{Q} = \eta_0, \quad (9)$$

identical with (4).

Turning to the high multiplicity case, the relation between the two-particle electromagnetic potential and the local charge density is given by

$$\nabla^2 \phi(\mathbf{r}) = -4\pi e(n^{(+)} - n^{(-)}), \quad (10)$$

where e is the elementary charge and where the density of charged mesons $n^{(\pm)}$ is then related to that of neutral mesons $n^{(0)}$ via a Boltzmann factor:

$$n^{(\pm)} = n^{(0)} \exp \left(\mp \frac{e\phi}{T} \right), \quad (11)$$

Here $n^{(0)}$ is the density of π^0 -mesons at the freeze-out temperature T , which coincides with the equilibrium density of charged pions in the absence of the Coulomb interaction (we consider symmetrical nuclear matter). When $e\phi \ll T$ the Eq.(11) can be rewritten as

$$n^{(\pm)} = n^{(0)} \left(1 \mp \frac{e\phi}{T} \right), \quad (12)$$

(this requires that the pions are not closer than $\sim 10^{-2}$ fm to one another at $T \approx 200$ MeV) so that

$$\nabla^2 \phi(\mathbf{r}) = \frac{4\pi e^2}{T} (2n^{(0)})\phi(\mathbf{r}), \quad (13)$$

where $e^2 = \alpha$.

We can write down immediately the well-known solution of the Eq.(13) as the screened Coulomb potential

$$\phi_{\pi^\pm}(r) = \pm e \frac{e^{-r/R_{scr}}}{r}, \quad (14)$$

where

$$\frac{1}{R_{scr}} = \sqrt{\frac{8\pi}{3}} \alpha \cdot \sqrt{\frac{n_\pi}{T}}, \quad (15)$$

with potential energy $U_{\pi\pi} = \alpha \exp(-r/R_{scr})/r$ for the like-sign pions.

To evaluate the correction to the Gamow factor, we will use this screened Coulomb potential to re-calculate the penetration parameter given by Eq.(5). This in turn requires an estimate of the pion density and freeze-out temperature. We will calculate this for the extreme case, i.e., just after freeze-out, when pions occupy the volume [7] (we take the same temperature $T_f = 190 \text{ MeV}$)

$$V_f = \pi R_f^2 2\tau_f \sinh \frac{\Delta y}{2} , \quad (16)$$

where for Pb-Pb collisions $R_f = R_{Pb} \approx 7.1 \text{ fm}$, $\tau_f = 10 \text{ fm}$ and $\Delta y \approx 6$. For multiplicities we assume [8]: *LHC*: $N_\pi = 8000$, *SPS*: $N_\pi = 800$, which gives for screening radii *LHC*: $R_{scr} = 7.9 \text{ fm}$, *SPS*: $R_{scr} = 25 \text{ fm}$. The latter looks rather controversial at first sight (though for a pure Coulomb interaction $R_{scr} = \infty$). Indeed, using Eq. (16) for the unit interval of rapidity (one might consider that more natural, in a sense) we obtain much smaller value of corresponding screening radius. None the less we cite this quantity here as an upper bound in existing experimental conditions.

The results of these calculations together with the standard Gamov factor are plotted in Fig. 1. Also shown there is a curve obtained by direct substitution of the experimental values obtained by NA44 [9] into Eq. (16), with $T_f = 187 \text{ MeV}$, $\tau_f = R_L \approx 6.0 \text{ fm}$, $R_T = 6 \text{ fm}$, $\Delta y = 3$ and $dN/dy = 40$. These parameters produce an even smaller screening radius ($R_{scr} = 19.3 \text{ fm}$) than our nominal SPS value (and hence a larger correction to the standard Gamov factor), which follows from the smaller values of $R_{scr} \approx 4\sqrt{T_f/n_\pi}$ at the NA44 experimental conditions. Based on these consideration alone, it would appear that a substantial correction to the Gamow factor is already required by the existing experimental data. This is particularly true for kaon interferometry since the pion medium screens the K-K Coulomb final state interaction as well, and the length scale for the K-K Gamov factor is larger than that for pions by the ratio of their masses.

However, it is important to note that correction factors presented in Fig. 1 are an upper bound, in that they do not incorporate the expansion of the pion source after freeze-out. We next turn to a more realistic calculation explicitly incorporating expansion. It is intuitively clear that the correction factor for the fast pairs will approach the standard Gamov factor and for the very slow ones the estimate obtained should be valid.

We parametrize the spherical expansion of the pion source

$$n(R) = n_f \frac{R_f^2}{R^2} , \quad (17)$$

in terms of the parameters n_f , the freeze-out pion density; the corresponding radius R_f and the freeze-out temperature T_f . In this model the spatial volume of the expanding pion system in the solid angle Ω increases as $\Omega \cdot R^2$, where R is the distance from the center of the fireball. Then, the corresponding potential is the solution of the Maxwell equation

$$(\nabla^2 - \partial_t^2) \phi(\mathbf{r}) = \frac{8\pi e^2}{3T} n_\pi \phi(\mathbf{r}) , \quad (18)$$

where we put $n^{(0)} \approx n_\pi/3$ as before. Now introducing the distance r between two detected particles we have

$$R \approx v_{cm} \cdot t , \quad r \approx v_{rel} \cdot t , \quad (19)$$

where v_{cm} is the velocity of the two-particle center-of-mass in the fireball rest frame and v_{rel} is the relative velocity of the particles ($v_{rel} = Q/m$, $t = 0$ is fixed on the freeze-out hyper-surface). Then

$$R = \frac{v_{cm}}{v_{rel}} \cdot r . \quad (20)$$

so that Eq.(18) may be rewritten as

$$\left(\nabla^2 - v_{rel}^2 \partial_r^2 \right) \phi(\mathbf{r}) = \frac{c^2(Q)}{r^2} \phi(\mathbf{r}) , \quad (21)$$

with $c^2(Q)$ defined as

$$c^2(Q) = \frac{8\pi e^2}{3} \frac{R_f^2 n_\pi}{T} \frac{v_{rel}^2}{v_{cm}^2} . \quad (22)$$

Fixing the screening radius at the freeze-out temperature and density as

$$R_{scr}^f = \sqrt{\frac{3T_f}{8\pi\alpha n_f}} , \quad (23)$$

we have

$$c(Q) = \frac{R_f}{R_{scr}^f} \frac{v_{rel}}{v_{cm}} . \quad (24)$$

and Eq.(18) can be rewritten as

$$r^2(1 - v_{rel}^2) \frac{d^2\phi}{dr^2} + 2r \frac{d\phi}{dr} - c^2(Q) \phi = 0 . \quad (25)$$

This equation has the following solution

$$\phi = \frac{e R_0^{a-1}}{r^a} , \quad (26)$$

where R_0 is a scale parameter to fix the dimensions of the potential ϕ . The exponent a is a solution of the quadratic equation resulting from the substitution of the ansatz (26) into Eq.(21) and takes the form (assuming proper asymptotic behaviour of the potential ϕ)

$$a = \frac{1}{2} \left[\frac{1 + v_{rel}^2}{1 - v_{rel}^2} + \sqrt{\left(\frac{1 + v_{rel}^2}{1 - v_{rel}^2} \right)^2 + \frac{4c^2(Q)}{1 - v_{rel}^2}} \right] , \quad (27)$$

For small pion relative velocity v_{rel} (corresponding to $Q \sim 0 - 30$ MeV) the above equation reduces to the simple expression

$$a = \frac{1}{2} + \frac{1}{2} \sqrt{1 + 4c^2(Q)} . \quad (28)$$

Both are shown for several sets of parameters in Fig. 2. In the interval of interest “ a ”, and hence deviations from a pure Coulomb field, increases with increasing relative velocity. This intriguing behavior is directly related to the “Hubble-like” expansion implied by Eq. (20), and becomes quite understandable if we remember that the pion density decreases (hence $R_{scr} \rightarrow \infty$) with R increasing. The expansion thus results in modifications to the Coulomb potential that are of power-law, not exponential form, in contrast to that static result given by Eq. (14). We can treat the corrected potential obtained in Eq.(26) in terms of an effective charge distribution

$$e_{eff} = e \left(\frac{R_0}{r} \right)^{a-1}, \quad (29)$$

which we are going to average over using the following procedure. If we confine our attention to $v_{rel} \ll 1$, Eq.(21) can be rewritten in a Poisson-like form $(\nabla^2 - \kappa^2)\phi(\mathbf{r}) = 0$, with $\kappa \equiv c(Q)/r$, which is equivalent to a r -dependent screening radius, i.e.,

$$R_{scr}(r) = \frac{r}{c(Q)}. \quad (30)$$

Since, as shown in Fig. 2, the deviation of the potential (26) from the pure Coulomb form in the region of small relative pion momenta $Q \leq 30 \text{ MeV}$ is small, we first ignore the r dependence of κ to obtain the solution for the electromagnetic $\pi\pi$ potential in the form of Eq. (14), then substitute the r -dependent κ into Eq. (14) to find

$$U_{\pi\pi} = \frac{\alpha e^{-c(Q)}}{r}, \quad (31)$$

Thus, there is no an exponential dependence of $U_{\pi\pi}$ on r . Instead, the numerator on r.h.s. of Eq.(31) represents the averaged charge distribution (29) squared (we are now considering the potential energy $U_{\pi\pi}$ rather than the electric potential ϕ , hence the extra factor of charge leading the α).

It is clear from Eq. (24) that when the ratio $v_{rel}/v_{cm} \ll 1$ (R_f and R_{scr}^f are of the same order for high multiplicities) the renormalized constant $\alpha \exp[-c(Q)]$ is close to the bare value of α . Moreover, the same qualitative result comes from the r -behaviour of the screening radius (30) when it approaches the asymptotic value $R_{scr} = \infty$ (Coulomb law) with increasing r . The quantity $c(Q)$ increases with relative pion momentum leading to larger deviations from the Coulomb potential and agreement with the features of the potential (26) (see discussion after Eq. (28)).

Based on these considerations, solving the Schrödinger equation for the screened potential gives results similar to Eqs. (3) and (4), but with the renormalized α , so that

$$\eta = \frac{\alpha m_\pi}{Q} \exp[-c(Q)] = \eta_0 \cdot \exp \left[-\frac{v_{rel}}{v_{cm}} \cdot \frac{R_f}{R_{scr}^f} \right], \quad (32)$$

and taking into account the Eq. (15) we have

$$\frac{R_f}{R_{scr}^f} = \sqrt{2\alpha \frac{N_\pi}{R_f T_f}}. \quad (33)$$

This result shows explicitly that the large modifications to the Gamow function from screening are weakened in the expansion model due to the small value of v_{rel}/v_{cm} . Specific examples of this are shown in Figs. 3 and 4.

Since for much of the parameter space $c(Q) \ll 1$, it is useful to further approximate $\exp[-c(Q)]$. Again referring to the NA44 data [9], and considering the direction transverse to the collision axis where $v_{cm} \approx p_T/m_T$ for the set of parameters

$$p_T \geq 150 \text{ MeV}/c, \quad N_\pi \leq 200, \quad R_f \geq 4 \text{ fm}, \quad T_f \geq 180 \text{ MeV}, \quad Q \leq 40 \text{ MeV}/c, \quad (34)$$

one has $\exp(-c(Q)) \simeq 1 - c(Q)$, and the screening of the Coulomb interaction reduces to shift η_0

$$\eta \simeq \eta_0 - \Delta\eta, \quad (35)$$

with

$$\Delta\eta = \alpha \frac{m_T}{p_T} \cdot \sqrt{2\alpha \frac{N_\pi}{T_f R_f}}, \quad (36)$$

being independent of relative pion momentum Q . (Clearly, for high multiplicities and for small p_T this approximation will be violated.)

For the case of cylindrical geometry we have

$$n_f = \frac{N_\pi}{\pi R_f^2 2\tau_f \sinh \frac{1}{2}\Delta y}. \quad (37)$$

and for the ratio (33)

$$\frac{R_f}{R_{scr}^f} = 2 \sqrt{\frac{\alpha}{3} \frac{N_\pi}{T_f \tau_f \sinh \frac{1}{2}\Delta y}}, \quad (38)$$

and finally

$$\eta = \eta_0 \cdot \exp \left[-\frac{2Qm_T}{p_T m_\pi} \sqrt{\frac{\alpha N_\pi}{3T_f \tau_f \sinh \frac{1}{2}\Delta y}} \right]. \quad (39)$$

Again, for the set of parameters where one might expect this geometry to apply,

$$p_T \geq 150 \text{ MeV}/c, \quad N_\pi \leq 2000, \quad \tau_f \geq 10 \text{ fm}, \quad \Delta y \geq 3, \quad T_f \geq 180 \text{ MeV}, \quad Q \leq 40 \text{ MeV}/c. \quad (40)$$

we obtain the shift $\Delta\eta$ as

$$\Delta\eta = 2\alpha \frac{m_T}{p_T} \cdot \sqrt{\frac{\alpha N_\pi}{3T_f \tau_f \sinh \frac{1}{2}\Delta y}}, \quad (41)$$

which is also independent of relative pion momentum.

Fig. 3 shows the role of screening for the correction factor G_{scr} behaviour evaluated at several sets of parameters together with the standard Gamov factor G_0 . Their ratio G_0/G_{scr} plotted in Figs. 4 and 5 show that correlators measured in the transverse direction develop a well-pronounced dependence on the transverse momentum of the pair in the region of $p_T \leq 150 \text{ MeV}/c$ [11] where the deviation from standard Gamov factor behaviour increases.

Our considerations show that for future LHC and RHIC experiments the screening radius of Coulomb interaction at the freeze-out density and temperature could be comparable with the source size and therefore the factorization of Eq. (2) [4] is no longer valid. However, this conclusion changes drastically with the inclusion (switching on) of expansion for the pion system. We would like to emphasize that this main result could be model independent. The detailed evaluation of the Gamow correction in pion interferometry analysis at very high multiplicities of secondary particles in the picture of an expanding fireball reveals an important regulating parameter what is the ratio of relative velocity of the detected pions and their center-of-mass velocity in the rest frame of a fireball v_{rel}/v_{cm} .

Acknowledgements: We would like to acknowledge useful conversations with D. Ferenc, G. Leksin, B. Lörstad, V. Lyuboshitz, L. McLerran, the late M. Podgoretsky, V. Ruuskanen, H. Satz, J. Schukraft and A. Stavinsky. One of us (D. A.) wishes to thank his colleagues at Physics Department of the University of Jyväskylä for their warm hospitality. This work was supported by INTAS Grant No.94-3941 and DOE FG02-86-ER40281.

References

- [1] A.D.Sakharov, Interaction of electron and positron during pair creation, Soviet JETP **18** (1948) 631-635.
- [2] V.N.Baier, V.S.Fadin, Coulomb final state interaction, Soviet JETP **57** (1969) 225-231, No.1(7).
- [3] D.H.Boal, C.-K.Gelbke and B.K.Jennings, Intensity interferometry in subatomic physics, Rev. Mod. Phys. **62** (1990) 553-602.
- [4] M.Gyulassy, S.K.Kauffmann and L.W.Wilson, Pion interferometry of nuclear collisions. I. Theory, Phys. Rev. **C20** (1979) 2267-2292.
- [5] A.Messiah, Quantum Mechanics Vol.1, North-Holland, Amsterdam 1961.
- [6] D.Anchishkin, G.Zinovjev, Two-pion correlation behavior in a small relative momentum region, Phys. Rev. **C51** (1995) No.5, pp.R2306-R2309.
- [7] Yu.M.Sinyukov, B.Lörstad, On intensity interferometry of high multiplicities, Z. Phys. **C61** (1994) 587-592.
- [8] H.Satz, In: Proc. LHC Workshop, vol. 1, CERN 90-10, Geneva 1990.
- [9] H.Atherton, H.Boggild, J.Boissevain et al., Results from CERN experiment NA44, Nucl. Phys. **A544** (1992) 125c-136c, Nos. 1,2.
- [10] G.F.Bertsch, Meson phase space density in heavy ion collisions from interferometry, Phys. Rev. Lett. **72** (1994) No. 15 pp.2349-2350.
- [11] H.Beker et al., m_T dependence of boson interferometry in heavy-ion collisions at the CERN SPS, CERN preprint CERN-PPE/94-119 (submitted to Phys. Rev. Lett.).

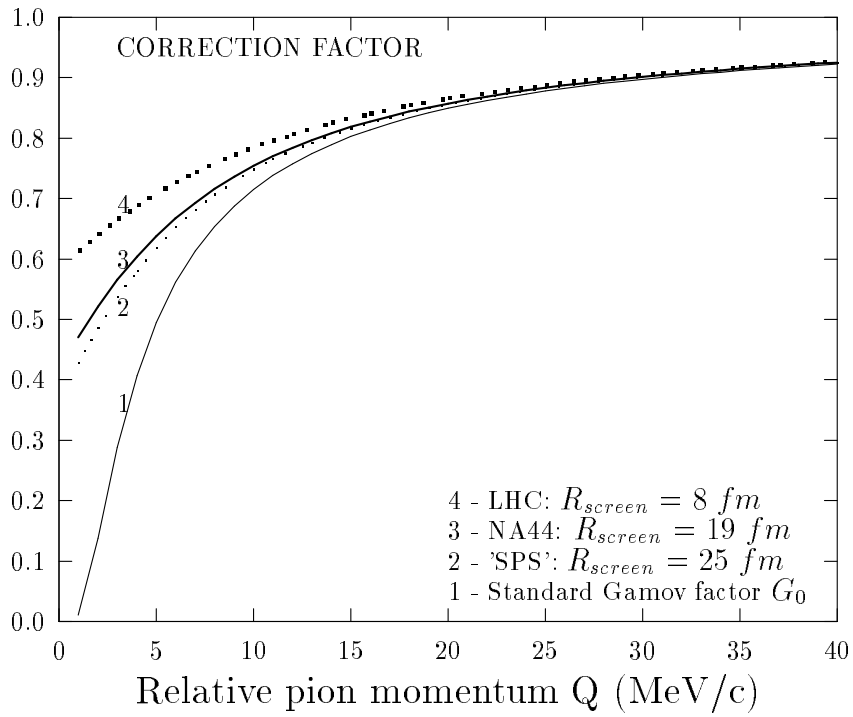


Figure 1. Extreme correction factors for screened Coulomb potential versus relative pion momentum. Bottom curve is the standard Gamov factor.

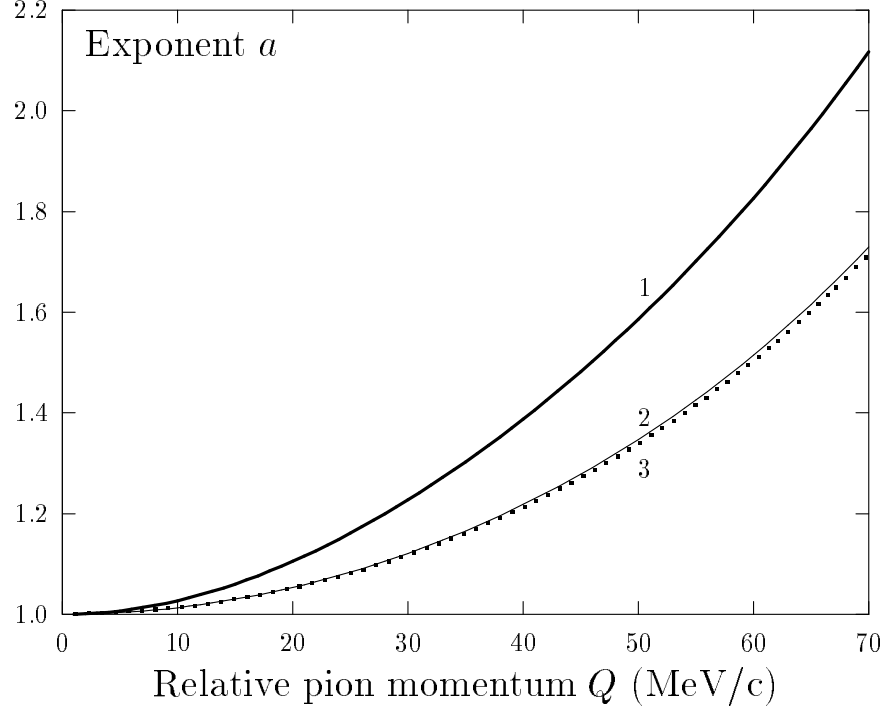


Figure 2a. Exponent a in the deformed Coulomb law $\phi(r) = eR_0^{a-1}/r^a$, which was calculated with taking into account the dependence of ϕ on time (see Eqs.(28) and (30)) for the following set of parameters:

1 - $R_f = 6 \text{ fm}$, $N_\pi = 1200$, $p_T = 450 \text{ MeV}/c$, $T_f = 190 \text{ MeV}$;

2 - $R_f = 6 \text{ fm}$, $N_\pi = 120$, $p_T = 150 \text{ MeV}/c$, $T_f = 187 \text{ MeV}$;

3 - $R_f = 4 \text{ fm}$, $N_\pi = 120$, $p_T = 450 \text{ MeV}/c$, $T_f = 190 \text{ MeV}$.

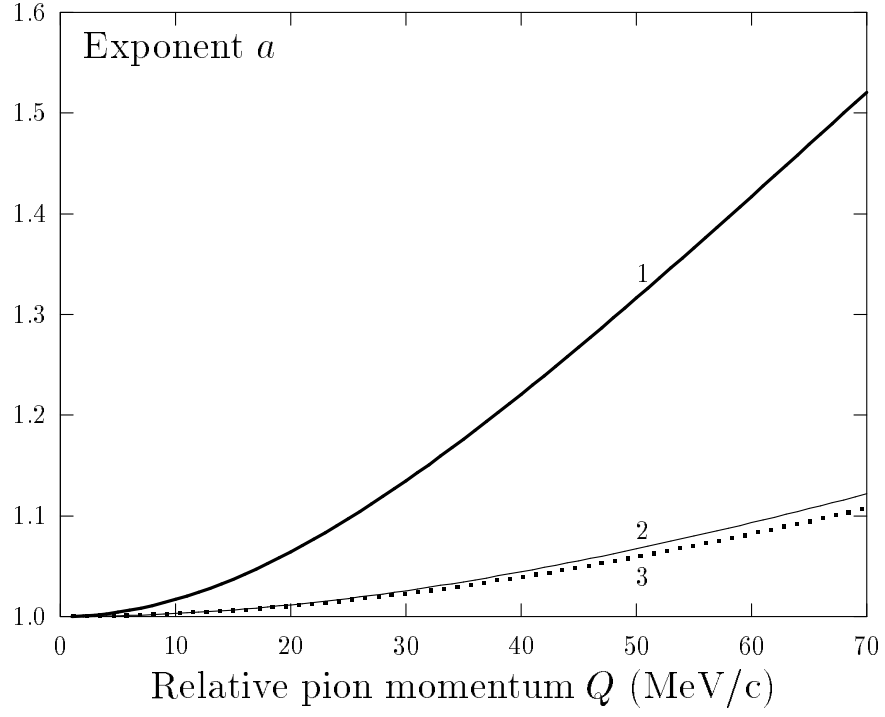


Figure 2b. Exponent a in the deformed Coulomb law $\phi(r) = eR_0^{a-1}/r^a$ which was calculated without taking into account the dependence of ϕ on time (see Eq.(31)) for the same as in Fig.2a set of parameters.

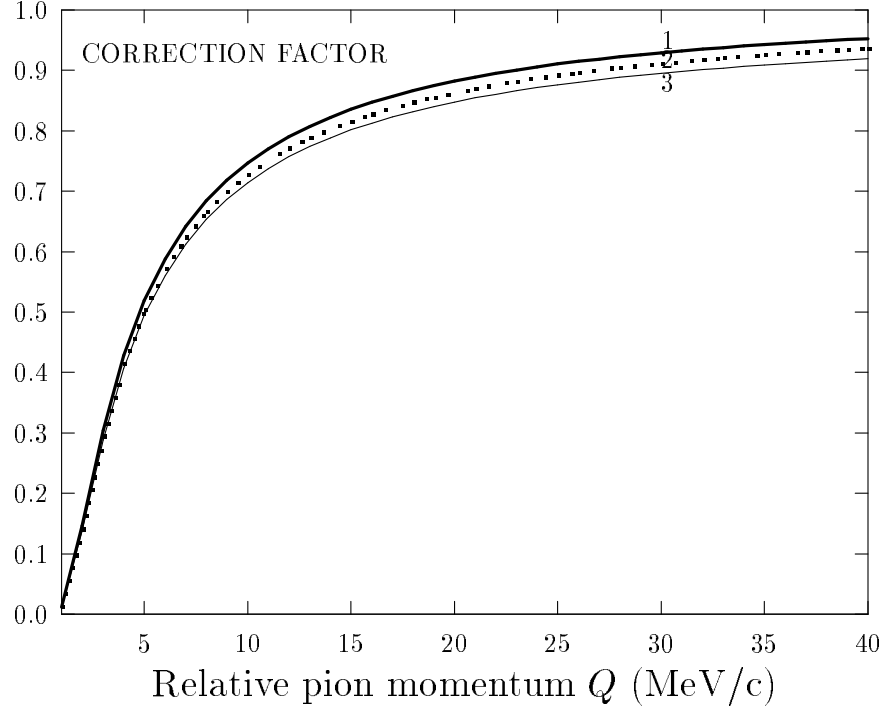


Figure 3. Correction factor for screened Coulomb potential versus relative pion momentum (expansion scenario). G_{scr} was evaluated for the set of parameters:

- 1 - $R_f = 6 \text{ fm}$, $N_\pi = 1200$, $p_T = 450 \text{ MeV}/c$, $T_f = 190 \text{ MeV}$;
- 2 - $R_f = 4 \text{ fm}$, $N_\pi = 120$, $p_T = 450 \text{ MeV}/c$, $T_f = 190 \text{ MeV}$;
- 3 - standard Gamov factor.

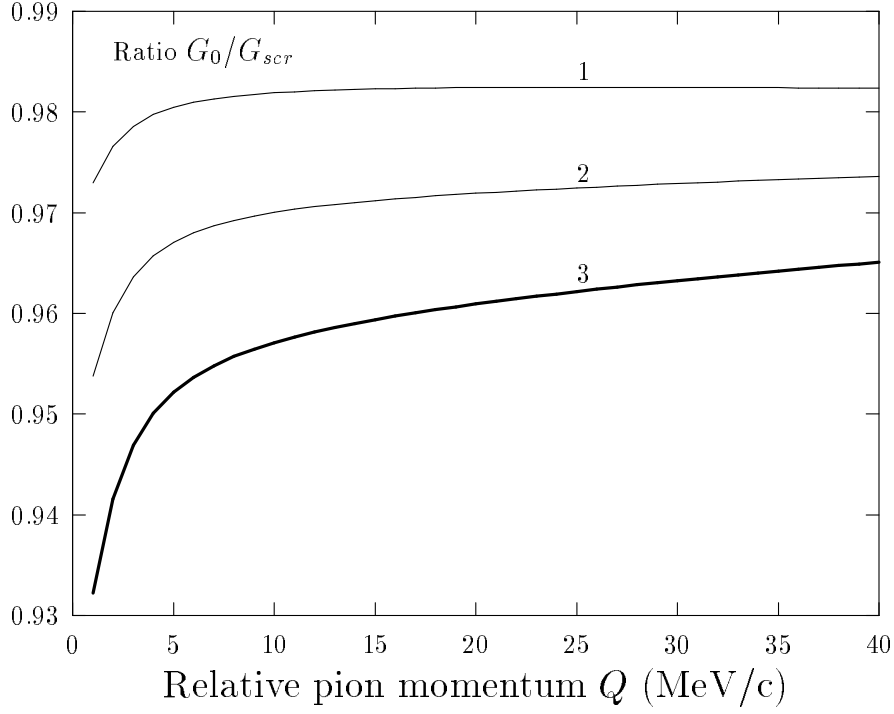


Figure 4. Ratio of the standard Gamov factor and correction factor for screened Coulomb potential versus relative pion momentum (expansion scenario). G_{scr} was evaluated for the set of parameters:

- 1 - $R_f = 4 \text{ fm}$, $N_\pi = 120$, $p_T = 450 \text{ MeV}/c$, $T_f = 190 \text{ MeV}$;
- 2 - LHC conditions $\tau_f = 10 \text{ fm}$, $N_\pi = 8000$, $p_T = 150 \text{ MeV}/c$, $\Delta y = 6$, $T_f = 190 \text{ MeV}$;
- 3 - $R_f = 6 \text{ fm}$, $N_\pi = 1200$, $p_T = 450 \text{ MeV}/c$, $T_f = 190 \text{ MeV}$.

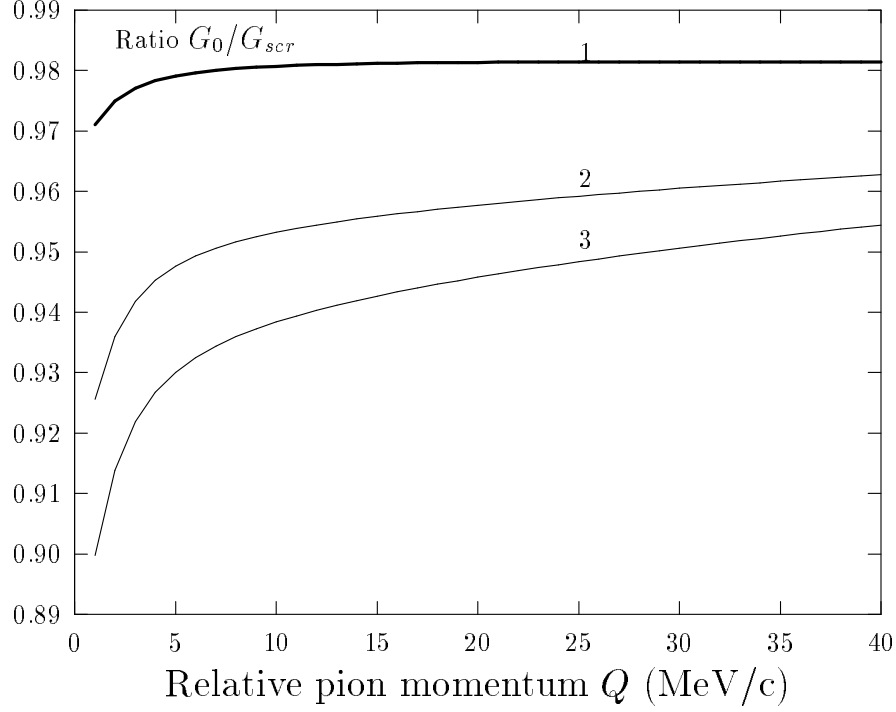


Figure 5. Ratio of the standard Gamov factor and correction factor for screened Coulomb potential versus relative pion momentum (expansion scenario). G_{scr} was evaluated for the set of parameters:

- 1 - $R_f = 6 \text{ fm}$, $N_\pi = 120$, $p_T = 150 \text{ MeV}/c$, $T_f = 187 \text{ MeV}$;
- 2 - $R_f = 4 \text{ fm}$, $N_\pi = 120$, $p_T = 50 \text{ MeV}/c$, $T_f = 187 \text{ MeV}$;
- 3 - $R_f = 3 \text{ fm}$, $N_\pi = 30$, $p_T = 20 \text{ MeV}/c$, $T_f = 187 \text{ MeV}$.